

RESEARCH PAPER

# Contrasting adaptation and optimization of stomatal traits across communities at continental scale

Congcong Liu<sup>1,2</sup>, Lauren Sack<sup>3</sup>, Ying Li<sup>1</sup>  and Nianpeng He<sup>1,2,\*</sup> 

<sup>1</sup> Key Laboratory of Ecosystem Network Observation and Modeling, Institute of Geographic Sciences and Natural Resources Research, Chinese Academy of Sciences, Beijing 100101, China

<sup>2</sup> College of Resources and Environment, University of Chinese Academy of Sciences, Beijing 100049, China

<sup>3</sup> Department of Ecology and Evolutionary Biology, University of California, Los Angeles, CA 90025, USA

\* Correspondence: [henp@igsnr.ac.cn](mailto:henp@igsnr.ac.cn)

Received 1 December 2021; Editorial decision 7 June 2022; Accepted 15 June 2022

Editor: Tracy Lawson, University of Essex, UK

## Abstract

Shifts in stomatal trait distributions across contrasting environments and their linkage with ecosystem productivity at large spatial scales have been unclear. Here, we measured the maximum stomatal conductance ( $g$ ), stomatal area fraction ( $f$ ), and stomatal space-use efficiency ( $e$ , the ratio of  $g$  to  $f$ ) of 800 plant species ranging from tropical to cold-temperate forests, and determined their values for community-weighted mean, variance, skewness, and kurtosis. We found that the community-weighted means of  $g$  and  $f$  were higher in drier sites, and thus, that drought ‘avoidance’ by water availability-driven growth pulses was the dominant mode of adaptation for communities at sites with low water availability. Additionally, the variance of  $g$  and  $f$  was also higher at arid sites, indicating greater functional niche differentiation, whereas that for  $e$  was lower, indicating the convergence in efficiency. When all other stomatal trait distributions were held constant, increasing kurtosis or decreasing skewness of  $g$  would improve ecosystem productivity, whereas  $f$  showed the opposite patterns, suggesting that the distributions of inter-related traits can play contrasting roles in regulating ecosystem productivity. These findings demonstrate the climatic trends of stomatal trait distributions and their significance in the prediction of ecosystem productivity.

**Keywords:** Adaptation, ecosystem productivity, forests, functional diversity, stomata, trait moments.

## Introduction

Stomata are epidermal structures formed by a pair of guard cells, and stomatal movements influence the exchange of water vapor and CO<sub>2</sub> between plants and the atmosphere (Edwards *et al.*, 1998; Hetherington and Woodward, 2003). The evolution of stomata was necessary for plants to colonize terrestrial ecosystems and the diversification of stomatal traits enables plants to inhabit a wide range of environments (Raven, 2002; Haworth *et al.*, 2011; Liu *et al.*, 2021a). The

numbers of stomatal pores, and their area and depth determine the anatomical maximum stomatal conductance ( $g$ ), which represent an anatomical constraint on the maximum rates of diffusion of carbon dioxide and water, and thereby their fluxes in given environments. There is a close relationship between  $g$  and field-measured stomatal conductance (McElwain *et al.*, 2016; Murray *et al.*, 2019; Xiong and Flexas, 2020), and  $g$  has been used to predict water vapor and CO<sub>2</sub> fluxes

(Franks and Beerling, 2009; McElwain *et al.*, 2016; Sack and Buckley, 2016). As  $g$  is strongly limited by the leaf epidermal space that is allocated to the stomata, the stomatal area fraction ( $f$ ) importantly constrains  $g$  (Franks and Beerling, 2009; de Boer *et al.*, 2016). Although many studies have found a close linkage between  $g$  and  $f$ , and some have thus proposed that  $f$  can be used as a proxy for  $g$  (Sack *et al.*, 2003; Holland and Richardson, 2009; Liu *et al.*, 2018), the similarity of their association with the environment and with ecosystem productivity has remained unclear. Here, we addressed this question by comparing the moments of stomatal trait distributions (community-weighted mean, variance, skewness, and kurtosis) across communities along a climatic transect.

A rich literature shows that contrasting trait values enable co-occurring species to exploit resources differentially across contrasting spatial or temporal scales (Hooper, 1998; Hooper *et al.*, 2005; Gross *et al.*, 2017). Indeed, traits that contribute to resource partitioning, such as root stratification (Schwendenmann *et al.*, 2015) or differential stomatal regulation (West *et al.*, 2012) can contribute not only to the mechanisms by which plants tolerate drought but also can improve species-specific soil moisture status by reducing competition for water among species. Given their importance in regulating gas exchange, and its coordination with other plant hydraulic traits (Sack *et al.*, 2003),  $g$  and its determinants may also be critical for the understanding of the adaptation of diverse species of communities across gradients of aridity. Generally, a higher  $g$  should benefit species under selection for high productivity or competition (Taylor *et al.*, 2012; Sack and Buckley, 2016), and thus, in communities with high water availability, we expected narrower functional niche differentiation of  $g$  than in communities of drier regions. Indeed, because plants can tolerate drought by maintaining low rates of water uptake and productivity as soils dry, i.e. 'tolerance', and/or by achieving their growth primarily when water is available, i.e. 'avoidance' (Grubb, 1998; Hetherington and Woodward, 2003), we hypothesized that community-weighted variance of  $g$  would tend to be larger in communities of drier regions. Notably,  $g$  can be considered as the product of  $f$  and  $e$  (the ratio of  $g$  to  $f$ , i.e. the maximum amount of CO<sub>2</sub> that can diffuse through a unit of stomatal area per unit time). Thus, a higher  $g$  represents a greater potential benefit in carbon assimilation rate, a higher  $f$  represents a greater cost of stomatal construction, maintenance and spatial allocation (de Boer *et al.*, 2016), and a higher  $e$  represents a greater benefit–cost ratio. We thus hypothesized that community-weighted variance of  $e$  within communities would be strongly constrained under water scarcity.

Stomatal traits may be a model for clarifying the role of plant traits in determining ecosystem functions, a priority topic in ecological research (Reichstein *et al.*, 2014). The effect of species' traits aggregated at ecosystem scale is typically quantified using the mass ratio hypothesis or the niche complementarity hypothesis (Liu *et al.*, 2021b). According to the mass ratio hy-

pothesis, the extent to which the trait of a given species affects ecosystem properties depends on its relative contribution to the total community biomass (Garnier *et al.*, 2004); supporting this hypothesis, many studies have found correlations between ecosystem functions and community-weighted mean (CWM) values of plant traits (Garnier *et al.*, 2004; Muscarella and Uriarte, 2016; Griffin-Nolan *et al.*, 2018). According to the niche complementarity hypothesis, resource niches may be used more completely when a community is functionally more diverse (Schumacher and Roscher, 2009); many studies have reported that ecosystem functions can be predicted by niche complementarity of traits, as quantified using community-weighted variance, skewness, or kurtosis of trait values (Gross *et al.*, 2017; Le Bagousse-Pinguet *et al.*, 2017; Zhang *et al.*, 2019; Liu *et al.*, 2020; Mensah *et al.*, 2020). Indeed, the community trait variance, skewness, and kurtosis provide information beyond the community weighted mean, which can overemphasize the role of dominant species (Enquist *et al.*, 2015). Specifically, the community variance in a given trait represents the functional divergence, skewness the asymmetry in the distribution of traits, and kurtosis the functional evenness, with a high kurtosis potentially indicating strong trait optimization (Umaña *et al.*, 2021). Yet, there is no clear consensus on how trait distributions scale up to influence productivity, and current global vegetation models typically predict ecosystem production based on the species mean values of traits.

Although stomatal traits are expected to influence ecosystem productivity, given their essential role in controlling leaf water and CO<sub>2</sub> fluxes (Hetherington and Woodward, 2003; Wang *et al.*, 2015), no studies have tested the relative importance of the distributions of stomatal traits (including community-weighted mean, variance, skewness, and kurtosis) in predicting ecosystem productivity across communities. We hypothesized a strong importance of these community distribution metrics for  $g$  and potentially for its components,  $f$  and  $e$ , for regulating ecosystem productivity at community scale. We analysed the community-weighted mean, variance, skewness, and kurtosis, and relationships among these statistical moments, for  $g$ ,  $f$ , and  $e$  for 800 plant species from nine sites along a climatic gradient and their relationships with environmental variables and ecosystem productivity, and tested three hypotheses: (i) the community-weighted variance in  $g$  would increase with aridity, due to variability in  $f$ , rather than  $e$ ; (ii) functional niche differentiation of  $g$  would be stronger for communities at higher aridity, consistent with the general assembly rule for maximization of trait diversity reported for specific leaf area and maximum plant height in drylands globally (Gross *et al.*, 2017); and (iii) that ecosystem productivity would be more strongly associated with community-weighted skewness and kurtosis of stomatal traits than with their community-weighted mean and variance (Le Bagousse-Pinguet *et al.*, 2021).

## Materials and methods

### Study sites and climate data

Nine study sites were selected along a 3700-km north–south transect of China (NSTEC): Huzhong, Liangshui, Changbai, Dongling, Taiyue, Shennongjia, Jiulian, Dinghu, and Jianfengling. The nine study sites extend from 18.7° N to 51.8° N latitude (Supplementary Fig. S1), and represent examples of most of the forest types in the northern hemisphere, including cold-temperate coniferous forest, temperate deciduous forest, subtropical evergreen forest, and tropical rain forest (He *et al.*, 2019). Along the NSTEC transect, the mean annual temperature (MAT) ranges from −3.67 to 23.2 °C, and mean annual precipitation (MAP) from 472 to 2266 mm (Supplementary Table S1). Soil types range from cold-temperate brown soils with high organic matter content to tropical red soils with low organic matter content (He *et al.*, 2020).

### Sample collection and analysis

The field survey was conducted in July–August 2013, the peak period of growth for all species. Sampling plots were located within well-protected national nature reserves with relatively continuous vegetation, which is representative of the given forests. Three or four experimental plots (30 m × 40 m) located least 100 m apart were established in each site. Geographical information (latitude, longitude, and altitude), plant species composition, and community structure were recorded for each plot. The number, height, diameter at breast height (DBH) of trees, basal stem diameter of shrubs, and aboveground live-biomass of all herbs were measured (He *et al.*, 2018).

Leaves were collected from trees, shrubs, and herbs within the plots. For each species, more than 20 mature leaves were collected from the top of the canopy of four healthy individuals and mixed as a composite sample. The leaves were collected from trees using long-handle shears or handpicked by climbing the trees. About half of the leaves were placed in sealed plastic bags, immediately stored in a box with ice, and the others were used to measure leaf morphological traits (Li *et al.*, 2018).

After sampling, leaf size was measured using a scanner (CanoScan LIDE 100, Canon, Japan) and Photoshop CS software (Adobe, USA). These leaves were subsequently dried to constant mass in an oven before measuring leaf dry mass, and specific leaf area as the ratio of leaf area to leaf dry mass. Eight to ten leaves from the pooled sample were cut into small pieces (1.0 × 0.5 cm) along the main vein and were fixed in 75% alcohol: formalin: glacial acetic acid: glycerol (90:5:5:5).

Stomatal traits were imaged using a scanning electron microscope (S-3400N, Hitachi, Japan), using the same leaf samples as previously studied for stomatal density, size, and stomatal area fraction (Liu *et al.*, 2018). Three small pieces were selected from the pooled sample, and each replicate was photographed twice on the lower surface at different positions. Given our use of scanning electron microscopy and investigation of a large number of species across communities, the labor and expense did not allow measurements of the upper epidermis, and we focused on the lower epidermis (Liu *et al.*, 2019). The herbaceous species in closed forests typically have more stomata on their adaxial surfaces, whereas trees and shrubs tend to have few or no stomata on the adaxial surface (Muir, 2015, 2018). Thus, sampling only the lower epidermis results in some uncertainty, but the community level findings are expected to be robust.

The number of stomata in each photograph was recorded, and stomatal density (SD) was calculated as the number of stomata per unit area (Liu *et al.*, 2018). In each photograph, five typical stomata were selected to measure stomatal length (SL), stomatal pore length (PL), and stomatal width (SW) by using MIPS (Optical Instrument Co., Ltd, Chongqing, China). Finally, SL, PL, and SW were measured 30 times for each species. We used the above stomatal traits to calculate  $f$  and  $g$  (Franks and Farquhar, 2001).

$$f = \frac{\pi}{4} \times \text{SD} \times \text{SW} \times \text{SL}$$

$$g = \text{SD} \times \left( \frac{D_w}{\nu} \right) \times \frac{a_{\max}}{l + 0.5(\pi a_{\max})^{0.5}}$$

where  $D_w$  is the diffusivity of water in air,  $\nu$  is the molar volume of water vapor,  $a_{\max}$  is the maximum pore area (estimated as the area of the ellipse with major axis PL and minor axis 0.5PL), and  $l$  is the depth of the stomatal pore, which was approximated as half stomatal width. We then calculated  $e$  as the ratio of  $g$  to  $f$ . Notably,  $e$  depends inversely on stomatal size, because smaller stomata, having shorter depths, are more efficient for transport for a given pore area (Franks and Farquhar, 2006).

### Stomatal trait moments of plant communities

To scale up traits to the community scale, and given that stomatal traits were normalized by leaf area, we used the total leaf area of each species in the plot to weight species trait values, and then calculated the distributions of stomatal traits. The total leaf biomass of each individual tree and shrub was calculated using species-specific allometric regressions based on measured values of height, diameter at breast height (DBH) or basal stem diameter, and then the leaf biomass of each species within plots was calculated. Species-specific allometric regressions were obtained from the Chinese Ecosystem Research Network (Zhang *et al.*, 2021). The above-ground biomass of the herb plot was measured using the harvest method. The total leaf area of each species was calculated as the product of total leaf biomass and specific leaf area. Community-weighted mean, variance, skewness, and kurtosis were calculated as follows (Gross *et al.*, 2017; Wiczyński *et al.*, 2019):

$$\text{Mean} = \sum_{i=1}^n p_i \text{Trait}_i$$

$$\text{Variance} = \sum_{i=1}^n p_i (\text{Trait}_i - \text{Mean})^2$$

$$\text{Skewness} = \sum_{i=1}^n \frac{p_i (\text{Trait}_i - \text{Mean})^3}{\text{Variance}^{3/2}}$$

$$\text{Kurtosis} = \sum_{i=1}^n \frac{p_i (\text{Trait}_i - \text{Mean})^4}{\text{Variance}^2}$$

where  $n$  is the species richness,  $p_i$  is the proportion of leaf area of  $i$ th plant species in a specific community, and  $\text{Trait}_i$  represents stomatal traits ( $g$ ,  $f$ , or  $e$ ) of the  $i$ th plant species.

Skewness and kurtosis are mathematically related, according to skewness–kurtosis relationships (SKR):

$$\text{Kurtosis} \geq \text{Skewness}^2 + 1$$

Thus, for a given skewness, there is a minimum kurtosis. Here, we calculated the distance between the observed kurtosis and minimum kurtosis (D):

$$D = \text{Kurtosis} - (\text{Skewness}^2 + 1)$$

$D$  signifies the extent to which functional diversity is maximized, with a  $D=0$  representing the strongest possible maximization of functional diversity (Gross et al., 2017).

#### Climate data and ecosystem productivity

MAT and MAP were derived from the Resource and Environment Data Cloud Platform (<http://www.resdc.cn/>). Then, the de Martonne aridity index (AI; de Martonne, 1926) was calculated as:

$$\text{AI} = \frac{\text{MAP}}{\text{MAT} + 10}$$

In these forests, gross primary productivity and net primary productivity were strongly correlated across sites (Li et al., 2020); here, we focused on gross primary productivity. The average gross primary productivity data from 2000 to 2015 (Li et al., 2020) were obtained from the Numerical Terradynamic Simulation Group (<http://www.ntsug.umd.edu/project/modis/mod17.php>). This dataset was derived from a widely used moderate resolution imaging spectroradiometer, and was calculated using the C5 MOD17 algorithm with data validation from flux towers (Zhao et al., 2005; Zhao and Running, 2010; Li et al., 2020).

#### Data analysis

We calculated statistical moments for stomatal traits, including mean, variance, skewness, and kurtosis, for each of the 32 plant community plots. We tested whether to consider plots independently, rather than as nested within sites, for calculating community scale moments by comparing fixed effects models (lm function in R) and mixed effects models (lmer function from R package lme4). The fixed model considered plots as independent, and the mixed effects models considered plots as a random factor nested within each site. The Akaike information criterion (AIC) represented the support of the model by data, with a model having a lower AIC value more likely to underlie the data (Burnham and Anderson, 2004). The AIC values of fixed and mixed effects models were compared, with differences greater than 2 considered decisive in selecting one model over another, representing a >100 times higher likelihood that the data were generated by that model. For 12 of the 13 relationships of traits with climate or ecosystem productivity tested in this study, the fixed effects model was selected (Supplementary Table S2–S6). Thus, in our analyses, we considered each plot as a sample plant community.

Pearson's correlation was used to test relationships between stomatal trait moments and climatic variables. Notably, there are inherent biases in using regression or correlation to test the relationship between CWM and environmental variables, and the fourth corner statistic can address these issues (Peres-Neto et al., 2012, 2017); thus, we also used the fourth corner method to explore stomatal trait–environment relationships. Ordinary least square regression was used to quantify relationships between statistical moments of stomatal traits, including the relationship between skewness<sup>2</sup> and kurtosis, and the relationship between variance and kurtosis. To explore whether climatic aridity mediated the relationships between variance and kurtosis, plant communities were classified into wet and dry communities (threshold AI=60), and scatter diagrams of variance and kurtosis were plotted.

The distance to the minimal kurtosis ( $D$ ) can be used to resolve the variation across communities in trait evenness (Gross et al., 2021). We tested the hypothesis that functional niche differentiation of  $g$  was greater in drier communities by determining the correlation between  $D$  and climatic aridity. To clarify whether stomatal trait assembly would maxi-

mize stomatal trait diversity, we tested whether observed SKRs differed from random expectations, which can reveal the signature of niche differentiation in shaping ecological communities (Gross et al., 2021). We constructed two null models, and predictions from each null model were derived from 2000 randomizations. In the first null model, we randomized the stomatal traits across all species, using the function 'richness' in the R package PICANTE (Kembel et al., 2010). In the second null model, we shuffled stomatal traits across species occurring in each community, using the function 'independentswap' in the R package PICANTE. These two null models have been the most common in analysing community assembly, with the second null model more specific in its implication. The first null model allows tests for whether trait diversity is maximized locally, relative to a scenario of random selection of species from the regional pool. The second null model allows tests for whether trait diversity is maximized locally relative to a scenario of random selection of species from local pools. Stomatal trait moments were then calculated for each of the 2000 randomizations, for each of the null models used. Then, we assessed whether the observed SKRs significantly differed from random expectations ( $\text{SKR}_{\text{random}}$ ) using Monte Carlo analysis. We compared the observed slope  $\beta$  and intercept  $\alpha$  ( $\beta_{\text{obs}}$  and  $\alpha_{\text{obs}}$ , respectively) of the SKR with those generated by null models ( $\beta_{\text{random}}$  and  $\alpha_{\text{random}}$ , respectively). Three pseudo  $P$ -values were calculated:  $P(\beta | \alpha)$ , the frequency of  $\beta_{\text{obs}} > \beta_{\text{random}}$  within subset  $\alpha_{\text{obs}} < \alpha_{\text{random}}$ ; the frequency of  $\alpha_{\text{obs}} > \alpha_{\text{random}}$  within subset  $\beta_{\text{obs}} < \beta_{\text{random}}$ ; and  $P(\beta \cap \alpha)$ , the frequency of  $\alpha_{\text{obs}} < \alpha_{\text{random}}$  within subset  $\beta_{\text{obs}} < \beta_{\text{random}}$ . Further, we compared the observed distance to the minimal kurtosis ( $D_{\text{obs}}$ ) with that generated by null models ( $D_{\text{random}}$ ).  $P(D)$  is the frequency of  $D_{\text{obs}} < D_{\text{random}}$ .

A multiple regression model was used to assess the potential influence of stomatal trait moments on ecosystem productivity, and the quadratic terms of stomatal trait moments were also considered as potential drivers of non-linear effects of these variables on ecosystem productivity. All variables, including ecosystem productivity and stomatal trait moments, were standardized (Z-scores) before analysis. We first used the 'stepAIC' function (MASS package in R) to exclude less important predictors, then the 'dredge' function (MuMIn package in R) was used to select the best models. Finally, the relative effect of each stomatal trait moment on ecosystem productivity was calculated as its absolute parameter compared with the sum of all the absolute parameters in the model.

Standardized effect sizes (SES) were used to assess the non-random influence of stomatal traits on ecosystem productivity. SES was calculated as

$$\text{SES} = \frac{\text{Adj. } r_{\text{obs}}^2 - \text{mean}(\text{Adj. } r_{\text{null}}^2)}{\text{SD}(\text{Adj. } r_{\text{null}}^2)}$$

Where adjusted  $r_{\text{obs}}^2$  is the observed influence of stomatal traits on ecosystem productivity, adjusted  $r_{\text{null}}^2$  is the influence of stomatal traits on ecosystem productivity of random communities generated from a null model, and SD is the standard deviation (Bruehlheide et al., 2018).

Data analyses and visualization were performed using R (<http://www.R-project.org/>). Statistical significance was set at the 0.05 level.

## Results

### Relationships between stomatal trait moments and climate

Stomatal traits were closely related to temperature, precipitation, and climatic aridity (Fig. 1). Overall, the relationships of community-weighted trait means and variances with climate variables were stronger than those of community-weighted skewness and kurtosis, and the aridity index was a stronger

predictor of stomatal traits than temperature and precipitation. The community-weighted means and variances of  $g$  and  $f$  were higher in drier sites, whereas for  $e$ , the community weighted variance was higher in wetter sites (Figs 1, 2). Additionally, using the fourth corner method, we also found both  $g$  and  $f$  were negatively correlated with AI (Supplementary Table S7).

We also tested the correlations between community-weighted variance and kurtosis (Supplementary Fig. S2). For  $g$  and  $f$ , the community-weighted variance and kurtosis were negatively correlated; such a correlation was not observed for  $e$ . At drier sites,  $g$  generally showed larger variance with lower kurtosis, whereas communities of wetter sites generally had smaller variance with a wide range of kurtosis.

### Skewness–kurtosis relationships and random expectations

In most cases, the distributions of stomatal traits differed substantially from normality (Fig. 3). The community-weighted skewness<sup>2</sup> and kurtosis of these three stomatal traits were strongly positively related. The skewness and kurtosis values generated by the null model were located within the constraint triangle imposed by the inequality  $\text{Kurtosis} \geq \text{Skewness}^2 + 1$ . The observed empirical SKRs for  $g$  deviated strongly from the predictions of the two null models, with the slopes ( $\beta$ ) higher and intercepts ( $\alpha$ ) lower than expected by chance, based on Monte Carlo analyses (Supplementary Table S8). The observed kurtosis values for both  $g$  and  $f$  were significantly closer than

expected by chance to the lower boundary of the mathematical constraint triangle. In other words, after controlling for the degree of skewness of  $g$  and  $f$ , observed kurtosis within communities was minimal. SKRs for  $e$  did not differ statistically from those generated by the two null models; thus, the  $D$  of  $e$  was not smaller than expected (Fig. 3).

Although the SKRs of  $g$  and  $f$  could not be explained by chance, the  $D$  of  $g$  and  $f$  was also influenced by climate. Specifically, drier communities had lower  $D$ -values for  $g$  and  $f$ , whereas for  $e$ , the  $D$ -value showed no climatic trends (Fig. 4).

### Stomatal trait moments and ecosystem productivity

The distributions of stomatal traits regulated ecosystem productivity (Fig. 5). The amount of variance in ecosystem productivity explained by community-weighted skewness and kurtosis was greater than that explained by community-weighted mean and variance. Community-weighted skewness and kurtosis of  $g$  and  $f$  played different roles in optimizing ecosystem productivity: if the other independent variables were fixed, increasing the skewness of  $f$  but decreasing that of  $g$ , and increasing the kurtosis of  $g$  but decreasing that of  $f$  would improve ecosystem productivity (Fig. 6). Further, ecosystem productivity increased across communities positively with the mean of  $e$ .

Overall stomatal traits explained up to 66% of the total variation observed in ecosystem productivity, which was greater than that explained by the distributions of stomatal traits generated by the two null models (Supplementary Fig. S3).

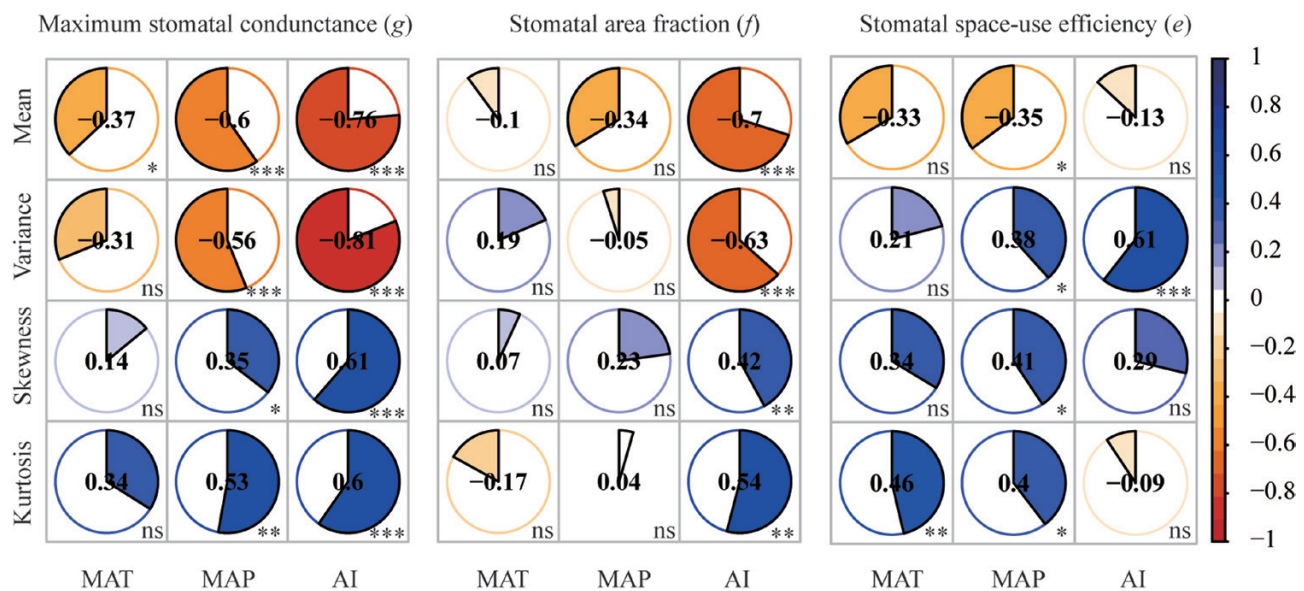


**Fig. 1.** Stomatal trait moments are broadly related to climatic aridity index. Mean, variance, skewness, and kurtosis are community-weighted values. Pearson's correlation coefficients are shown in the panels. Fan-shaped areas are proportional to the absolute Spearman rank correlation coefficients; negative correlations are drawn with a counterclockwise fan and positive correlations with a clockwise fan. The strength of negative correlation increases from white to red, and the strength of positive correlation increases from white to blue. ns, not significant at the 0.05 level; \* $P < 0.05$ ; \*\* $P < 0.01$ ; \*\*\* $P < 0.001$ . CI, climatic aridity index; MAP, mean annual precipitation; MAT, mean annual temperature.

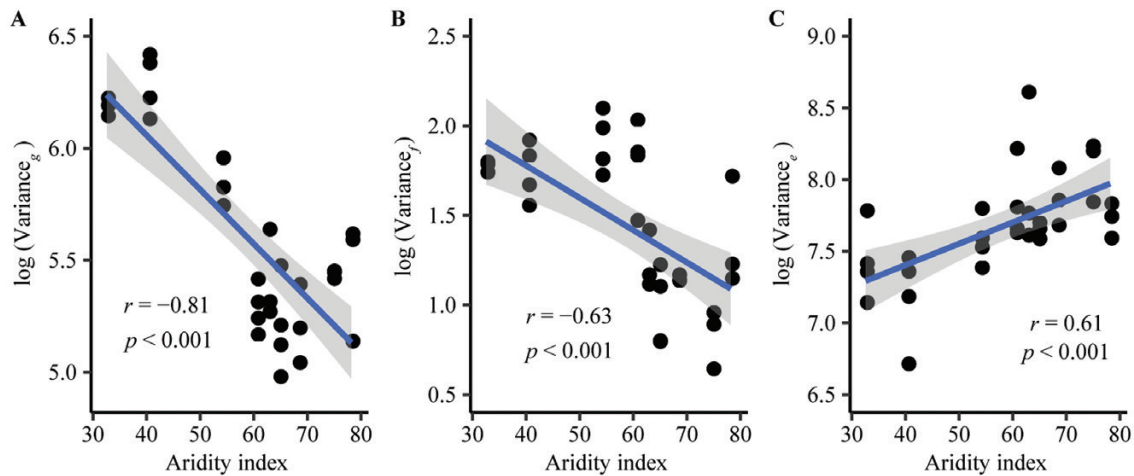


**Fig. 2.** Relationships between the community-weighted variance of stomatal traits and climatic aridity index. Variance is community-weighted. *e*, stomatal space-use efficiency; *f*, stomata area fraction; *g*, maximum stomatal conductance. The blue lines were fitted using linear regression, and shaded areas indicate the 95% confidence interval.

## Discussion

### *Maximum stomatal conductance (g) increases with climatic aridity at continental scale*

The linkage of *g* with low water availability has remained controversial. Previous work has shown that plants may adapt to dry conditions with a low *g* that may enable sustained low rates of gas exchange under extended periods of lower water supply, with increased CO<sub>2</sub> gain relative to water loss, i.e. higher water use efficiency (Franks *et al.*, 2015). However, other studies have proposed a higher *g* and stomatal conductance can confer an advantage for plants in arid climates, enabling greater rates of photosynthesis in the shorter ‘pulses’ when water is available (Grubb, 1998; Scoffoni *et al.*, 2011; Wang *et al.*, 2017), thus ‘avoiding’ drought with opportunistic rapid growth during short periods of water availability. One of the major novel findings of this study was that the community-weighted mean value of *g* was positively related to climatic aridity across the continent (Fig. 1), and thus that pulse-driven ‘avoidance’ is the dominant trend for adaptation of communities with low water availability. Our findings extend to a continental scale the hypothesis that plants and communities adapted to arid climates would generally maintain a low stomatal conductance, but given their high maximum stomatal conductance, can sharply increase stomatal conductance during pulses of rainfall availability to maximize growth (Grubb, 1998). This hypothesis is also consistent with reports that species with higher *g* tend to show greater sensitivity to changes in the external environment (Siddiq *et al.*, 2017; Haworth *et al.*, 2018).

### *Greater functional niche differentiation of g under higher climatic aridity*

Environmental stress can restrict the variance of trait values, leading to convergence in the distribution of trait values

among co-existing species (Kraft *et al.*, 2008). Yet, for communities across a continental scale aridity gradient, the community-weighted variance of *g* increased with climatic aridity (Fig. 2). Notably, this difference for *g* would be expected due to the ability of plants to close stomata; species with a high *g* are not obliged to maintain high stomatal conductance during stressful periods, as species with large stomatal pore areas can sharply reduce stomatal conductance and thus transpiration rates. The distance between observed kurtosis and minimum kurtosis (*D*) for *g* was lower than that generated by two null models (Supplementary Table S1; Fig. 3), consistent with a general assembly rule that trait diversity of *g* is maximized within forest plant communities, as previously demonstrated for global drylands in analyses of specific leaf area and maximum height (Gross *et al.*, 2017). Further, the *D* values of *g* were lower for drier communities (Fig. 4), suggesting that this assembly rule applies more strongly with increasing aridity. Similarly to root stratification (Oram *et al.*, 2018), diversity in *g* and associated stomatal regulation strategies might improve species-specific soil moisture status (West *et al.*, 2012) and increase species partitioning of water resources in space and/or time, thus increasing overall water utilization (Naem *et al.*, 1994). We observed a negative relationship between community-weighted variance and kurtosis of *g* (Supplementary Fig. S1); communities characterized by low variance and low kurtosis values were only observed in the wetter regions, indicating that the community assembly process of *g* was more strictly constrained under lower water availability. The strong patterns linking the stomatal traits of communities with climate at continental scale highlights the importance of these traits across the background of other structural and physiological adaptations to aridity, including specialized xylem anatomy, plant allometry, rooting strategy, dormancy, and the ability to recover after dieback (Grossiord, 2020).

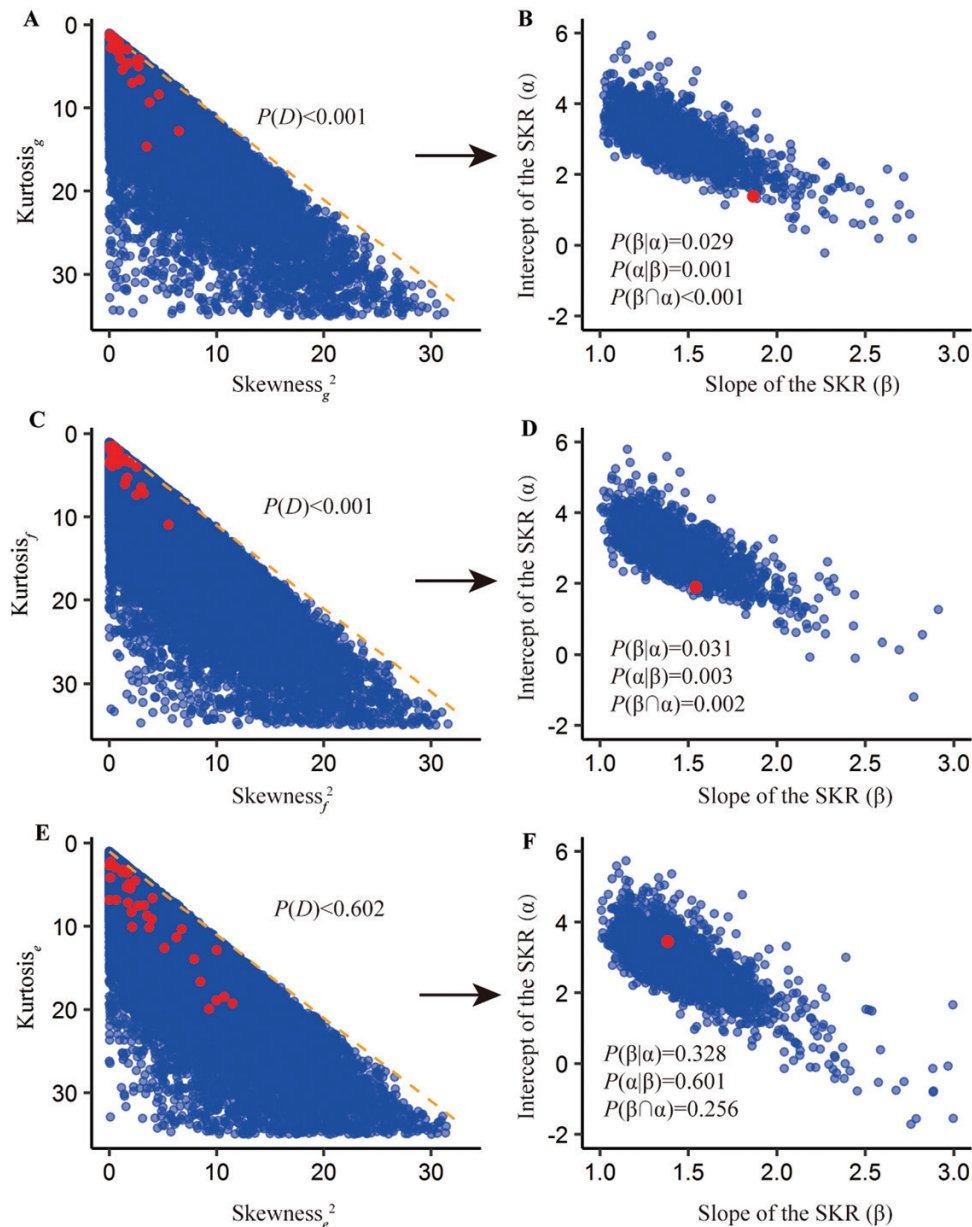


**Fig. 3.** Observed skewness–kurtosis relationships (SKR) and deviation from null expectations. Skewness, community-weighted skewness; Kurtosis, community-weighted kurtosis. *e*, stomatal space-use efficiency; *f*, stomatal area fraction; *g*, maximum stomatal conductance. The red dots in the left panels represent the observed skewness and kurtosis values; blue dots in the left panels represent the skewness and kurtosis values of simulated random communities. The orange line represents  $y=x+1$ . Red/blue dots in the right panels represent the observed/random slope ( $\alpha$ ) and intercept ( $\beta$ ) of the SKRs. We indicate the conditional pseudo *P*-values from null model ‘richness’ for the slope  $\beta$ ,  $P(\beta|\alpha)$ ; the  $y$ -intercept  $\alpha$ ,  $P(\alpha|\beta)$ ; the whole model,  $P(\beta \cap \alpha)$ ; and the distance to the lower boundary,  $P(D)$  (see [Supplementary Table S6](#) for details).

#### Limited variability of stomatal space-use efficiency under water scarcity

Stomatal space-use efficiency (*e*) was first defined in this study, and, by contrast with *g* and *f*, community-weighted mean values of *e* were not statistically constrained by climatic aridity (Fig. 4), supporting the theory that this efficiency should be generally maximized (Franks and Beerling, 2009). For *g* and *f*, the overall negative correlation of community-

weighted mean trait values with aridity was consistent with the expected trends based on adaptation (Grime, 1998; Garnier *et al.*, 2004; Garnier and Navas, 2012). Likewise, given that community-weighted mean values of *e* were highly conservative, the relatively narrow community-weighted variance of *e* would reflect adaptation in which co-occurring species tend to converge in *e* to a narrow range of optimal values. Our results support the hypothesis that the variability

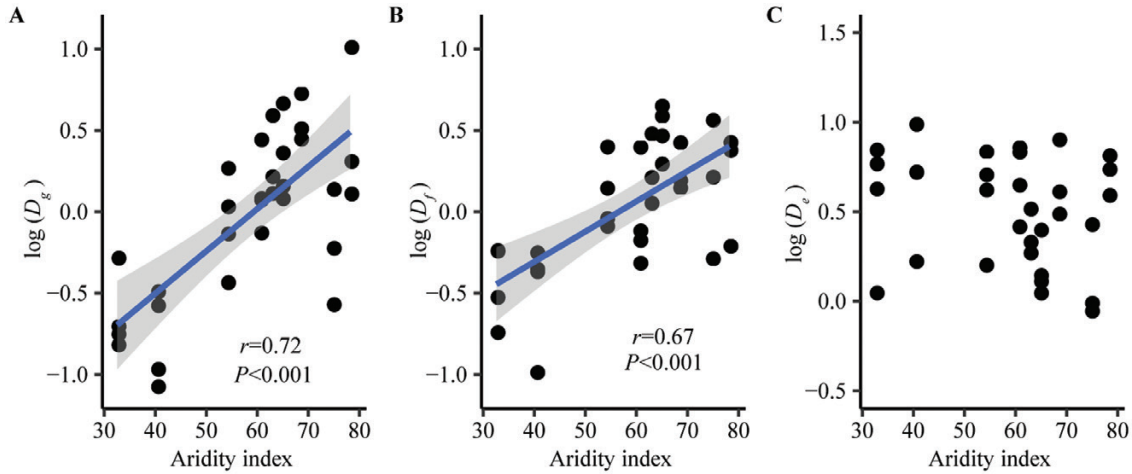


**Fig. 4.** Relationships between the distance to the lower boundary ( $D$ ) and climatic aridity index.  $e$ , stomatal space-use efficiency;  $f$ , stomatal area fraction;  $g$ , maximum stomatal conductance. The blue lines were fitted using linear regression and the shaded areas indicate the 95% confidence interval.

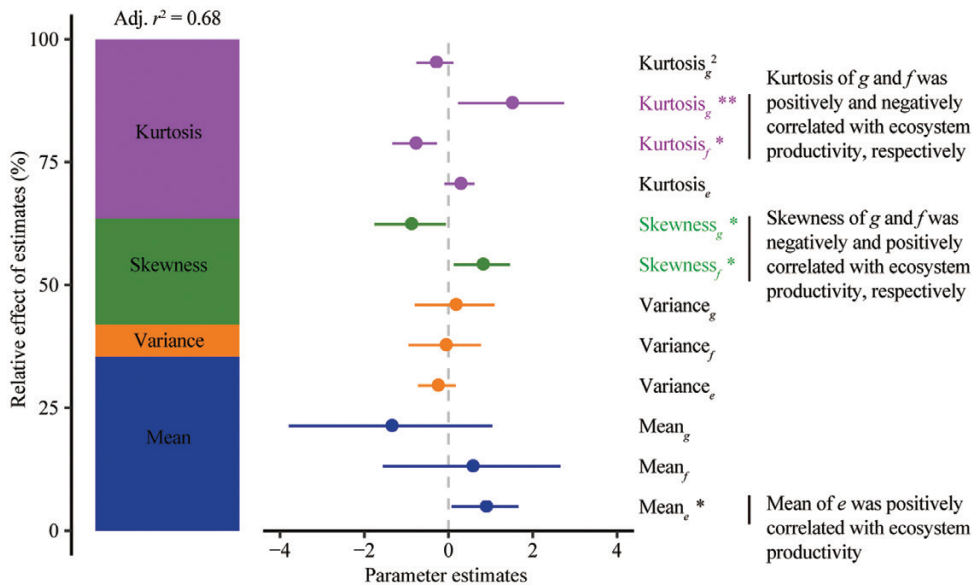


**Fig. 5.** Community-weighted skewness and kurtosis of  $g$  and  $f$  showed opposite effects on ecosystem productivity. Mean, variance, skewness, and kurtosis, were community-weighted.  $e$ , stomatal space-use efficiency;  $f$ , stomatal area fraction;  $g$ , maximum stomatal conductance. Average parameter estimates (standardized regression coefficients) of model predictors, associated 95% confidence intervals, and relative importance of each factor are expressed as the percentage of explained variance. Colored labels in the right highlighted the different effects of  $g$  and  $f$  on ecosystem productivity. \* $P < 0.05$ ; \*\* $P < 0.01$ .

of  $e$  was especially strongly constrained under arid climates, consistent with the expectation of greater cost-effectiveness of investment in stomata under lower water availability than under high water availability, where selection would likely be weaker.

### Coordinated adaptation of $g$ and $f$ across a climatic gradient

For both  $g$  and  $f$ , the community-weighted mean and variance increased with the climatic aridity, whereas  $D$  decreased,

and the trait diversity was maximized. Thus, the distributions of  $g$  and  $f$  were synchronous in adaptation to the environment. Given that  $g$  is determined as the product of  $f$  and  $e$ , and that variation in  $g$  was primarily determined by  $f$  rather than  $e$ , it is clear that the shifts in stomatal area fraction are more typical for the adaptation and assembly of  $g$  than shifts in  $e$ , which remains constrained. As  $e$  is inversely proportional to stomatal size, its constraint is consistent with previous studies reporting that stomatal size is less variable than stomatal density or  $f$  (Beaulieu et al., 2008; Jordan et al., 2015; Xiong and Flexas, 2020).

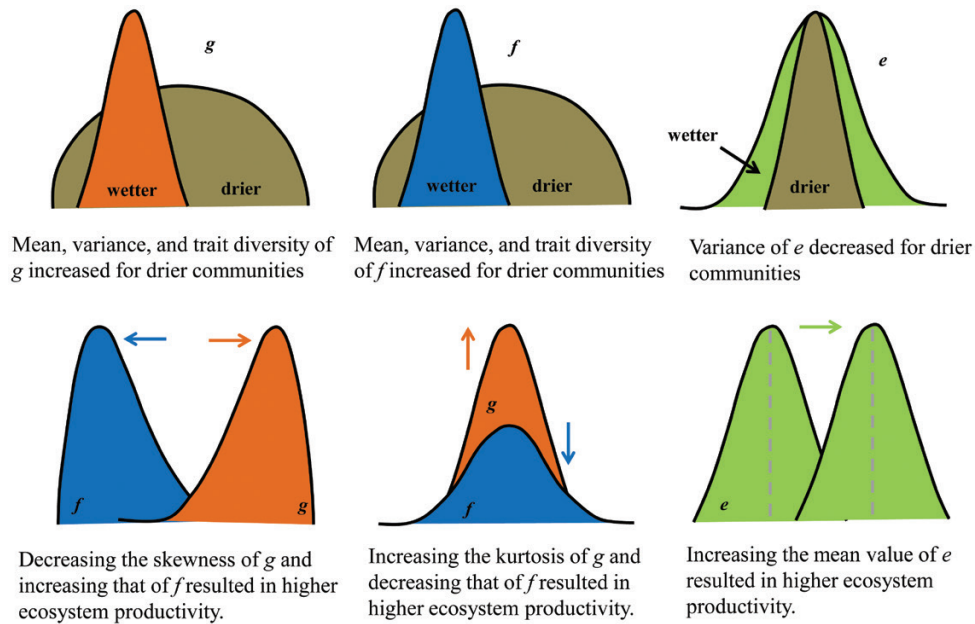


**Fig. 6.** Maximum stomatal conductance and stomatal area fraction were convergent in adaptation but divergent in their influences on productivity across communities along a climatic aridity gradient.  $e$ , stomatal space-use efficiency, shown in green;  $f$ , stomatal area fraction, shown in blue;  $g$ , maximum stomatal conductance, shown in orange.

### Contrasting roles of $g$ and $f$ in optimizing ecosystem productivity

The evolution of stomatal morphology tends to follow allometric relationships that minimize  $f$  (the cost) as plants evolve towards higher  $g$  (the benefit) (de Boer *et al.*, 2016), and such cost–benefit optimization also influences how stomatal traits regulate ecosystem productivity. Higher productivity was achieved for communities with greater dominance of species with higher  $g$  and lower  $f$  values (Fig. 5), such that these communities had lower skewness of  $g$  and greater skewness of  $f$ . We also found that increasing the kurtosis of  $g$  and decreasing the kurtosis of  $f$  would improve the ecosystem productivity, which further demonstrated their different roles at the community level (Fig. 6). A previous study also argued that high kurtosis in leaf traits indicated strong trait optimization (Umaña *et al.*, 2021). The high kurtosis of  $g$  meant that co-occurring species were convergent toward an optimal value of  $g$ , in other words, optimization of stomatal benefit would improve ecosystem productivity, yet the negative relationship between kurtosis of  $f$  and ecosystem productivity was hard to interpret. Nevertheless, our study demonstrated contrasting regulation of ecosystem productivity by  $g$  and  $f$ , according to the stomatal cost–benefit relationship, which was further supported by the positive relationship between  $e$  (the benefit–cost ratio) and ecosystem productivity.

We note that the causal role of stomatal traits in determining ecosystem productivity requires further investigation, as this is not conclusively established by their correlation and mutual association with climate. Indeed, considering the relationships

of plant traits and ecosystem productivity, it is not clear which is the cause and which is the effect; Li *et al.* (2020) interpreted leaf size as a driver of ecosystem productivity whereas Moles *et al.* (2009) interpreted ecosystem productivity as the driver of the global pattern of height. Yet, given the well-established roles of stomata in controlling leaf water and  $\text{CO}_2$  fluxes at leaf level, the hypothesis that this control scales up to an important influence on ecosystem productivity is supported by our findings.

### Conclusions

We provide the first analyses of stomatal trait moments including mean, variance, skewness, and kurtosis across communities at a regional scale. The results demonstrated that under increasingly arid climates, the stomatal space-use efficiency ( $e$ ) of plants tended to converge in community-weighted means, whereas species varied increasingly in their allocation to stomatal area fraction, resulting in functional niche differentiation of  $g$ . Across all communities,  $g$  and  $f$  were similar in characterizing plant adaptation, but differed in regulating ecosystem productivity, indicating that future studies should be cautious in using  $f$  as an equivalent of  $g$  for comparisons at community or continental scale.

### Supplementary data

The following supplementary data are available at [JXB online](#).  
Fig. S1. Geographic distribution of sampling sites.

Fig. S2. Relationships between community-weighted variance and community-weighted kurtosis of stomatal traits.

Fig. S3. Observed effect of stomatal traits on ecosystem productivity (Adj.  $r^2$ ) and null expectations.

Table S1. Location and key properties of nine contrasting forests.

Table S2. Comparison of fixed effects and mixed effects models for testing relationships between community-weighted mean of stomatal traits and climatic aridity index.

Table S3. Comparison of fixed effects and mixed effects models for testing relationships between community-weighted variance of stomatal traits and climatic aridity.

Table S4. Comparison of fixed effects and mixed effects models for testing relationships between community-weighted skewness and community-weighted kurtosis.

Table S5. Comparison of fixed effects and mixed effects models for testing relationships between the distance between observed kurtosis and minimum kurtosis (Distance) and climatic aridity index.

Table S6. Comparison of fixed effects and mixed effects models for testing relationships between stomatal trait moment and ecosystem gross primary productivity (GPP).

Table S7. Stomatal trait–environment relationships revealed by the fourth corner method.

Table S8. Results from the null model for stomatal traits.

## Acknowledgements

We thank the staff in nine forest ecosystem research stations for access to their study sites.

## Author contributions

NH planned and designed the research; CL and YL conducted fieldwork and collected data; CL, LS, and YL analysed data and wrote the manuscript; LS and CL revised the manuscript.

## Conflict of interest

The authors declare no conflicts of interest.

## Funding

This work was supported by National Natural Science Foundation of China [31988102, 42141004, 32171544], the national science and technology basic resources survey program of China [2019FY101300], a fellowship of China Postdoctoral Science Foundation [2020M680663, 2021M693147, 2021M703186], and the United States National Science Foundation [Grant 2017949].

## Data availability

The stomatal trait distribution data underlying this paper are available at <https://doi.org/10.5061/dryad.w6m905qr2> (Liu *et al.*, 2022).

## References

- Beaulieu JM, Leitch IJ, Patel S, Pendharkar A, Knight CA. 2008. Genome size is a strong predictor of cell size and stomatal density in angiosperms. *New Phytologist* **179**, 975–986.
- Bruelheide H, Dengler J, Purschke O, *et al.* 2018. Global trait–environment relationships of plant communities. *Nature Ecology & Evolution* **2**, 1906–1917.
- Burnham KP, Anderson DR. 2004. Multimodel inference: understanding AIC and BIC in model selection. *Sociological Methods & Research* **33**, 261–304.
- de Boer HJ, Price CA, Wagner-Cremer F, Dekker SC, Franks PJ, Veneklaas EJ. 2016. Optimal allocation of leaf epidermal area for gas exchange. *New Phytologist* **210**, 1219–1228.
- de Martonne E. 1926. L'indice d'aridité. *Bulletin de l'Association des Géographes Français* **9**, 3–5.
- Edwards D, Kerp H, Hass H. 1998. Stomata in early land plants: an anatomical and ecophysiological approach. *Journal of Experimental Botany* **49**, 255–278.
- Enquist BJ, Norberg J, Bonser SP, Violle C, Webb CT, Henderson A, Sloat LL, Savage VM. 2015. Chapter Nine. Scaling from traits to ecosystems: developing a general trait driver theory via integrating trait-based and metabolic scaling theories. *Advances in Ecological Research* **52**, 249–318.
- Franks PJ, Beerling DJ. 2009. Maximum leaf conductance driven by CO<sub>2</sub> effects on stomatal size and density over geologic time. *Proceedings of the National Academy of Sciences, USA* **106**, 10343–10347.
- Franks PJ, Doheny-Adams T W, Britton-Harper ZJ, Gray JE. 2015. Increasing water-use efficiency directly through genetic manipulation of stomatal density. *New Phytologist* **207**, 188–195.
- Franks PJ, Farquhar GD. 2001. The effect of exogenous abscisic acid on stomatal development, stomatal mechanics, and leaf gas exchange in *Tradescantia virginiana*. *Plant Physiology* **125**, 935–942.
- Franks PJ, Farquhar GD. 2006. The mechanical diversity of stomata and its significance in gas-exchange control. *Plant Physiology* **143**, 78–87.
- Garnier E, Cortez J, Billès G, *et al.* 2004. Plant functional markers capture ecosystem properties during secondary succession. *Ecology* **85**, 2630–2637.
- Garnier E, Navas M-L. 2012. A trait-based approach to comparative functional plant ecology: concepts, methods and applications for agroecology. A review. *Agronomy for Sustainable Development* **32**, 365–399.
- Griffin-Nolan RJ, Bushey JA, Carroll CJW, *et al.* 2018. Trait selection and community weighting are key to understanding ecosystem responses to changing precipitation regimes. *Functional Ecology* **32**, 1746–1756.
- Grime JP. 1998. Benefits of plant diversity to ecosystems: immediate, filter and founder effects. *Journal of Ecology* **86**, 902–910.
- Gross N, Le Bagousse-Pinguet Y, Liancourt P, Berdugo M, Gotelli NJ, Maestre FT. 2017. Functional trait diversity maximizes ecosystem multifunctionality. *Nature Ecology & Evolution* **1**, 0132.
- Gross N, Le Bagousse-Pinguet Y, Liancourt P, Saiz H, Violle C, Munoz F. 2021. Unveiling ecological assembly rules from commonalities in trait distributions. *Ecology Letters* **24**, 1668–1680.
- Grossiord C. 2020. Having the right neighbors: how tree species diversity modulates drought impacts on forests. *New Phytologist* **228**, 42–49.
- Grubb PJ. 1998. A reassessment of the strategies of plants which cope with shortages of resources. *Perspectives in Plant Ecology, Evolution and Systematics* **1**, 3–31.
- Haworth M, Elliott-Kingston C, McElwain JC. 2011. Stomatal control as a driver of plant evolution. *Journal of Experimental Botany* **62**, 2419–2423.
- Haworth M, Scutt CP, Douthe C, Marino G, Gomes MTG, Loreto F, Flexas J, Centritto M. 2018. Allocation of the epidermis to stomata relates to stomatal physiological control: Stomatal factors involved in the evolutionary diversification of the angiosperms and development of amphistomaty. *Environmental and Experimental Botany* **151**, 55–63.

- He N, Li Y, Liu C, et al.** 2020. Plant trait networks: Improved resolution of the dimensionality of adaptation. *Trends in Ecology & Evolution* **35**, 908–918.
- He N, Liu C, Piao S, et al.** 2019. Ecosystem traits linking functional traits to macroecology. *Trends in Ecology & Evolution* **34**, 200–210.
- He N, Liu C, Tian M, Li M, Yang H, Yu G, Guo D, Smith MD, Yu Q, Hou J.** 2018. Variation in leaf anatomical traits from tropical to cold-temperate forests and linkage to ecosystem functions. *Functional Ecology* **32**, 10–19.
- Hetherington AM, Woodward FI.** 2003. The role of stomata in sensing and driving environmental change. *Nature* **424**, 901–908.
- Holland N, Richardson AD.** 2009. Stomatal length correlates with elevation of growth in four temperate species. *Journal of Sustainable Forestry* **28**, 63–73.
- Hooper DU.** 1998. The role of complementarity and competition in ecosystem responses to variation in plant diversity. *Ecology* **79**, 704–719.
- Hooper DU, Chapin FS III, Ewel JJ, et al.** 2005. Effects of biodiversity on ecosystem functioning: A consensus of current knowledge. *Ecological Monographs* **75**, 3–35.
- Jordan GJ, Carpenter RJ, Koutoulis A, Price A, Brodrribb TJ.** 2015. Environmental adaptation in stomatal size independent of the effects of genome size. *New Phytologist* **205**, 608–617.
- Kembel SW, Cowan PD, Helmus MR, Cornwell WK, Morlon H, Ackerly DD, Blomberg SP, Webb CO.** 2010. Picante: R tools for integrating phylogenies and ecology. *Bioinformatics* **26**, 1463–1464.
- Kraft NJ, Valencia R, Ackerly DD.** 2008. Functional traits and niche-based tree community assembly in an Amazonian forest. *Science* **322**, 580–582.
- Le Bagousse-Pinguet Y, Gross N, Maestre FT, Maire V, de Bello F, Fonseca CR, Kattge J, Valencia E, Leps J, Liancourt P.** 2017. Testing the environmental filtering concept in global drylands. *Journal of Ecology* **105**, 1058–1069.
- Le Bagousse-Pinguet Y, Gross N, Saiz H, et al.** 2021. Functional rarity and evenness are key facets of biodiversity to boost multifunctionality. *Proceedings of the Royal Society B: Biological Sciences* **118**, e2019355118.
- Li Y, Liu C, Zhang J, Yang H, Xu L, Wang Q, Sack L, Wu X, Hou J, He N.** 2018. Variation in leaf chlorophyll concentration from tropical to cold-temperate forests: Association with gross primary productivity. *Ecological Indicators* **85**, 383–389.
- Li Y, Reich PB, Schmid B, et al.** 2020. Leaf size of woody dicots predicts ecosystem primary productivity. *Ecology Letters* **23**, 1003–1013.
- Liu C, He N, Zhang J, Li Y, Wang Q, Sack L, Yu G.** 2018. Variation of stomatal traits from cold temperate to tropical forests and association with water use efficiency. *Functional Ecology* **32**, 20–28.
- Liu C, Li Y, Xu L, Chen Z, He N.** 2019. Variation in leaf morphological, stomatal, and anatomical traits and their relationships in temperate and subtropical forests. *Scientific Reports* **9**, 5803.
- Liu C, Li Y, Xu L, Li M, Wang J, Yan P, He N.** 2021a. Stomatal arrangement pattern: A new direction to explore plant adaptation and evolution. *Frontiers in Plant Science* **12**, 655255.
- Liu C, Li Y, Yan P, He N.** 2021b. How to improve the predictions of plant functional traits on ecosystem functioning? *Frontiers in Plant Science* **12**, 622260.
- Liu C, Li Y, Zhang J, Baird AS, He N.** 2020. Optimal community assembly related to leaf economic-hydraulic-anatomical traits. *Frontiers in Plant Science* **11**, 341.
- Liu C, Sack L, Li Y, He N.** 2022. Data from: Contrasting adaptation and optimization of stomatal traits across communities at continental scale. Dryad Digital Repository. <https://doi.org/10.5061/dryad.w6m905qr2>
- McElwain JC, Yiotis C, Lawson T.** 2016. Using modern plant trait relationships between observed and theoretical maximum stomatal conductance and vein density to examine patterns of plant macroevolution. *New Phytologist* **209**, 94–103.
- Mensah S, Salako KV, Assogbadjo A, Kakai RG, Sinsin B, Seifert T.** 2020. Functional trait diversity is a stronger predictor of multifunctionality than dominance: Evidence from an Afromontane forest in South Africa. *Ecological Indicators* **115**, 106415.
- Moles AT, Warton DI, Warman L, Swenson NG, Laffan SW, Zanne AE, Pitman A, Hemmings FA, Leishman MR.** 2009. Global patterns in plant height. *Journal of Ecology* **97**, 923–932.
- Muir CD.** 2015. Making pore choices: repeated regime shifts in stomatal ratio. *Proceedings of the Royal Society B: Biological Sciences* **282**, 20151498.
- Muir CD.** 2018. Light and growth form interact to shape stomatal ratio among British angiosperms. *New Phytologist* **218**, 242–252.
- Murray M, Soh WK, Yiotis C, Spicer RA, McElwain JC.** 2019. Consistent relationship between field-measured stomatal conductance and theoretical maximum stomatal conductance in C<sub>3</sub> woody angiosperms in four major biomes. *International Journal of Plant Sciences* **181**, 142–154.
- Muscarella R, Uriarte M.** 2016. Do community-weighted mean functional traits reflect optimal strategies? *Proceedings of the Royal Society B: Biological Sciences* **283**, 20152434.
- Naeem S, Thompson LJ, Lawler SP, Lawton JH, Woodfin RM.** 1994. Declining biodiversity can alter the performance of ecosystems. *Nature* **368**, 734–737.
- Oram NJ, Ravenek JM, Barry KE, et al.** 2018. Below-ground complementarity effects in a grassland biodiversity experiment are related to deep-rooting species. *Journal of Ecology* **106**, 265–277.
- Peres-Neto PR, Dray S, ter Braak CJF.** 2017. Linking trait variation to the environment: critical issues with community-weighted mean correlation resolved by the fourth-corner approach. *Ecography* **40**, 806–816.
- Peres-Neto PR, Leibold MA, Dray S.** 2012. Assessing the effects of spatial contingency and environmental filtering on metacommunity phylogenetics. *Ecology* **93**, S14–S30.
- Raven JA.** 2002. Selection pressures on stomatal evolution. *New Phytologist* **153**, 371–386.
- Reichstein M, Bahn M, Mahecha MD, Kattge J, Baldocchi DD.** 2014. Linking plant and ecosystem functional biogeography. *Proceedings of the National Academy of Sciences, USA* **111**, 13697–13702.
- Sack L, Buckley TN.** 2016. The developmental basis of stomatal density and flux. *Plant Physiology* **171**, 2358–2363.
- Sack L, Cowan PD, Jaikumar N, Holbrook NM.** 2003. The ‘hydrology’ of leaves: co-ordination of structure and function in temperate woody species. *Plant, Cell & Environment* **26**, 1343–1356.
- Schumacher J, Roscher C.** 2009. Differential effects of functional traits on aboveground biomass in semi-natural grasslands. *Oikos* **118**, 1659–1668.
- Schwendenmann L, Pendall E, Sanchez-Bragado R, Kunert N, Hölscher D.** 2015. Tree water uptake in a tropical plantation varying in tree diversity: interspecific differences, seasonal shifts and complementarity. *Ecohydrology* **8**, 1–12.
- Scoffoni C, Rawls M, McKown A, Cochard H, Sack L.** 2011. Decline of leaf hydraulic conductance with dehydration: Relationship to leaf size and venation architecture. *Plant Physiology* **156**, 832–843.
- Siddiq Z, Chen Y-J, Zhang Y-J, Zhang J-L, Cao K-F.** 2017. More sensitive response of crown conductance to VPD and larger water consumption in tropical evergreen than in deciduous broadleaf timber trees. *Agricultural and Forest Meteorology* **247**, 399–407.
- Taylor SH, Franks PJ, Hulme SP, Spriggs E, Christin PA, Edwards EJ, Woodward FI, Osborne CP.** 2012. Photosynthetic pathway and ecological adaptation explain stomatal trait diversity amongst grasses. *New Phytologist* **193**, 387–396.
- Umaña MN, Arellano G, Swenson NG, Zambrano J.** 2021. Tree seedling trait optimization and growth in response to local-scale soil and light variability. *Ecology* **102**, e03252.
- Wang H, Prentice IC, Keenan TF, Davis TW, Wright IJ, Cornwell WK, Evans BJ, Peng C.** 2017. Towards a universal model for carbon dioxide uptake by plants. *Nature Plants* **3**, 734–741.
- Wang R, Yu G, He N, Wang Q, Zhao N, Xu Z, Ge J.** 2015. Latitudinal variation of leaf stomatal traits from species to community level in forests: linkage with ecosystem productivity. *Scientific Reports* **5**, 14454.
- West AG, Dawson TE, February EC, Midgley GF, Bond WJ, Aston TL.** 2012. Diverse functional responses to drought in a Mediterranean-type shrubland in South Africa. *New Phytologist* **195**, 396–407.

**Wieczynski DJ, Boyle B, Buzzard V, et al.** 2019. Climate shapes and shifts functional biodiversity in forests worldwide. *Proceedings of the National Academy of Sciences, USA* **116**, 587–592.

**Xiong D, Flexas J.** 2020. From one side to two sides: the effects of stomatal distribution on photosynthesis. *New Phytologist* **228**, 1754–1766.

**Zhang D, Peng Y, Li F, Yang G, Wang J, Yu J, Zhou G, Yang Y.** 2019. Trait identity and functional diversity co-drive response of ecosystem productivity to nitrogen enrichment. *Journal of Ecology* **107**, 2402–2414.

**Zhang J, Li M, Xu L, Zhu J, Dai G, He N.** 2021. C:N:P stoichiometry in terrestrial ecosystems in China. *Science of the Total Environment* **795**, 148849.

**Zhao M, Heinsch FA, Nemani RR, Running SW.** 2005. Improvements of the MODIS terrestrial gross and net primary production global data set. *Remote Sensing of Environment* **95**, 164–176.

**Zhao M, Running SW.** 2010. Drought-induced reduction in global terrestrial net primary production from 2000 through 2009. *Science* **329**, 940–943.